Catalysis Letters
https://doi.org/10.1007/s10562-020-03206-y

Microporous Polymeric Spheres as Highly Efficient and Metal-Free Catalyst for the Cycloaddition of CO_2 to Cyclic Organic Carbonates at Ambient Conditions

Shunmin Ding[1] · Ling Sun[1] · Xiaohua Ma[1] · Dan Cheng[1] · Shaohua Wu[1] · Rong Zeng[2] · Shengjun Deng[1] · Chao Chen[1] · Ning Zhang[1]

Received: 6 February 2020 / Accepted: 1 April 2020

Abstract

The cycloaddition of CO_2 with epoxides to cyclic organic carbonates using metal-free heterogeneous catalysts is considered as a 100% atom-economic and environmental-friendly route for CO_2 utilization. Herein, we developed a metal-free microporous polymeric spheres catalyst (*p*-TBIB) by a simple Friedel–Crafts alkylation and applied in the cycloaddition of CO_2 to cyclic organic carbonates. The catalyst shows high CO_2 uptake (62.7 $cm^3\ g^{-1}$, at 298 K and 1 bar), high selectivity over N_2 (46 at 298 K) and perfect cycloaddition activities (66–97%) and selectivities (over 99%) and reusability (at least ten cycles) at ambient conditions (at 298 K and 1 bar).

Graphic Abstract

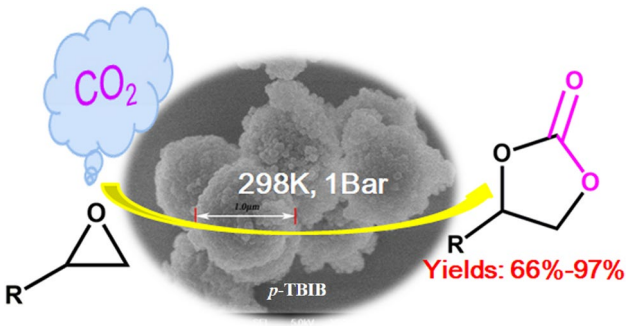

Keywords Carbon dioxide · Cyclic organic carbonates · Heterogeneous catalysis · Microporous polymeric spheres · Metal-free

1 Introduction

Carbon dioxide (CO_2) emission is widely recognized as a main cause of greenhouse effect that leads to global warming. Concurrently, it is also regarded as an attractive renewable carbon resource with abundant, nontoxic, cheap, and nonflammable nature [1–3]. In recent years, numerous pioneering studies have been undertaken on the utilization of CO_2 to high-value organic products. In terms of "environmental-friendly chemistry" and "atom economy", the cycloaddition of CO_2 with epoxides is a promising route to

Electronic supplementary material The online version of this article (https://doi.org/10.1007/s10562-020-03206-y) contains supplementary material, which is available to authorized users.

✉ Shunmin Ding
dingshunmin2007@163.com

✉ Rong Zeng
zengrongnc@163.com

✉ Chao Chen
chaochen@ncu.edu.cn

Extended author information available on the last page of the article

Published online: 04 April 2020

produce cyclic organic carbonates, which are widely used as aprotic polar solvents, electrolytes, monomers for polymers, fine chemical intermediates, etc. [4–6].

In the past decades, numerous homogeneous catalysts [5–15] such as organocatalysts [5, 7, 8], metal salen complexes [6, 9–11] and metalloporphyrins complexes [12–15] are developed for this purpose. Although some of them exhibit high activities for the reaction, the catalysts are not easily separated from the catalytic system and reused. To solve the drawback, heterogeneous catalysts especially porous materials based heterogenous catalysts [16–24], such as nanoporous polymers, nanoporous polymers metalled catalysts and metalorganic frameworks (MOFs) have been developed. Though the heterogeneous catalysts are ease of purification and recycle, most of them perform under rigorous temperatures, drastic CO_2 pressures. Only a few heterogeneous catalysts [17–23] (Co/POP-TPP [17], Co(III)@cage [18], Hf-NU-1000 [19], Cu-MOF [20–22] and Co-CMP [23]) have the ability for converting CO_2 into cyclic carbonates under mild conditions such as at room temperature and atmospheric pressure, which typically need metal ions (e.g. Cu^{2+} and Co^{2+}). However, the metal ions can be leached into the catalytic system to pollute the products. Hence, developing novel, stable and highly efficient metal-free heterogeneous catalysts for the cycloaddition of CO_2 with epoxides under mild and even ambient conditions is still a big challenge.

In industrial production, cyclic carbonates are prepared under high CO_2 pressure (5 MPa) to ensure adequate CO_2 reaction concentration [25]. In general, the CO_2 concentration of CO_2 emission is lower than 15% [26]. So the CO_2 capacity and selectivity of a catalyst is one of the key factors to the reaction rate for the cycloaddition of CO_2 with epoxides. Recently, Porous organic polymers (POPs) have been focused on as an ideal CO_2 absorbent because of their large specific surface areas, high pore volumes, and abundant functional groups. The POPs including covalent organic frameworks (COFs) [27, 28], conjugated microporous polymers (CMPs) [29] and hyper-crosslinked polymers (HCPs) [30] usually show high CO_2 capacity and selectivity. The stability of the POPs is one of the most important aspects for their industrial applications such as in catalysis and CO_2 selective capture. Various nanostructured POPs have been synthesized. Among them, spherical POPs have attracted tremendous attention over the past decade. Because objects in nature tend to approach minimum energy, spherical structure is one of the most perfect structures for matter, having the smallest surface-to-volume ratio, which is an optimal shape by nature selection [31].

To design a perfect POPs catalyst for the cycloaddition of CO_2 with epoxides with high activity, the selection of active moieties is the key. In previous works, the active moieties such as containing hydrogen bond donor groups (e.g., −OH, −NH) can activate epoxides by hydrogen bond, and facilitating ring opening and subsequent CO_2 insertion [32–36]. Although the −OH and −NH can easily open the ring of epoxides, most of them require high temperature or pressure due to the low CO_2 concentration in the liquid phase. Therefore, how to improve CO_2 concentration in the reaction system and the epoxides ring opening ability is the two aspect of designing a high catalyst for the reaction.

Herein, we design and synthesize a 1,3,5-tris(*1H*-benzo[d]imidazol-2-yl)benzene-linked polymeric spheres catalyst (*p*-TBIB, Scheme 1) with imidazole units (containing –NH bonds), high CO_2 capacity of 100.8 $cm^3\ g^{-1}$ (62.7 $cm^3\ g^{-1}$) and CO_2/N_2 selectivity of 37 (46) under 1 bar at 273 K (298 K), respectively. As expected, the catalyst exhibits very good conversions and cyclic organic carbonates yields under ambient conditions with a perfect reusability (at least ten cycles).

2 Experimental

2.1 Materials

All starting materials and solvents, unless otherwise noted, were obtained from Acros Organics and used without further purification. Trimesic acid, 1,2-diaminobenzene were purchased from Adamas and used without further purification. Phosphoric acid was purchased from Damao Chemical Regents Co. Ltd. Dichloromethane and aluminum chlorides were purchased from Sinopharm Chemical Regents Co. Ltd. The dichloromethane was dried over CaH_2 and freshly distilled prior to use.

2.2 Synthesis of 1,3,5-tris(*1H*-benzo[d]imidazol-2-yl)benzene (TBIB)

We modified the synthesis process of the literature [37]. The detail procedure was given in supporting information.

2.3 Synthesis of 1,3,5-tris(*1H*-benzo[d]imidazol-2-yl)benzene-linked polymeric spheres (*p*-TBIB)

Under N_2 gas protection, TBIB (200 mg, 0.47 mmol) was dissolved in anhydrous dichloromethane (10 mL). The solution was subsequently added dropwise to a mixture of anhydrous $AlCl_3$ (400 mg, 3.00 mmol) and anhydrous dichloromethane (20 mL). The resulting mixture was heated to 80 °C and kept string under N_2 atmosphere for 24 h. After the reaction completed, it was cooled and quenched with methanol (10 mL) in an ice-water bath. The obtained polymer was washed with ethanol, 5% HCl, and DI-water. The solid was further purified using Soxhlet extraction with

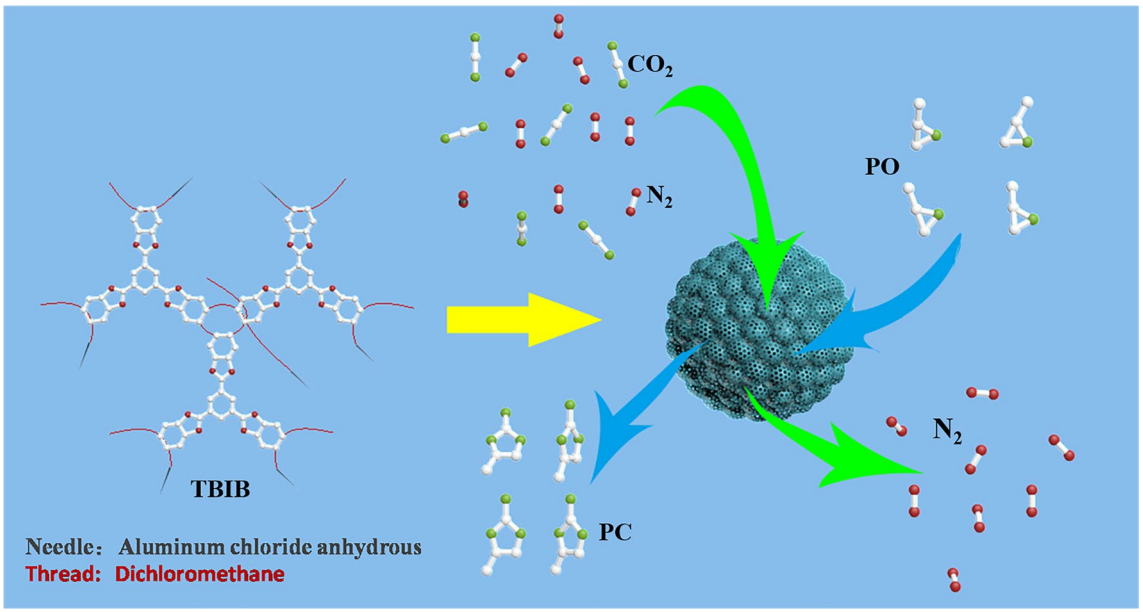

Scheme 1. The synthetic route to *p*-TBIB

methanol for 24 h and then with tetrahydrofuran for another 24 h. Finally, the desired tawny polymer was collected and dried in a vacuum oven at 80 °C overnight. For comparison, PTPB was prepared with the same method.

2.4 Characterization

Nitrogen sorption was measured on a Micro ASAP 2020 adsorption instrument at 77 K. FT-IR spectra were recorded on a Nicolet 5700 instrument. X-ray diffraction (XRD) measurements were performed on a XD-3 diffractometer with Cu Kα radiation (λ = 0.15418 nm, 40 kV/30 mA) at a scanning step of 2° min^{-1}. Thermogravimetric analysis (TGA) was carried out using a TA Instruments Q-5000IR series thermal gravimetric analyzer with samples under nitrogen at a heating rate of 10 °C min^{-1}. X-ray photoelectron spectroscopy (XPS) was performed on an ESCALAB250xi spectrometer (Thermon Scientific), all binding energies were calibrated by using the C 1*s* peak at 284.8 eV as a reference. ^{1}HNMR spectra were recorded on an Agilent 400 MHz instrument using TMS as the internal standard. Cross polarized magic angle spinning (CP/MAS) solid state nuclear magnetic resonance (SSNMR) spectrum was recorded using Bruker Avance III-500 spectrometer. Scanning electron microscope (SEM) images were collected on a Zeiss Auriga Crossbeam SEM at an acceleration voltage of 5 kV.

2.5 CO_2 and N_2 adsorption

CO_2 and N_2 adsorption isotherms at 273 and 298 K were also measured on a Micromeritics ASAP 2020 system. Prior to the measurement, *p*-TBIB was dried at 393 K under high vacuum (0.1 Pa) for 48 h. Isosteric heat of CO_2 adsorption (Q_{st}) was calculated according to the Clausius–Clapeyron equation by fitting CO_2 isotherms (273 and 298 K) with virial equation.

2.6 Catalytic cycloaddition of CO_2 with epoxides

In a typical reaction, a mixture of epoxide (5 mmol), tetrabutylammonium bromide (TBAB) (37.5 mg 2.34 mol% relative to epoxide), *n*-dodecane (1 mL, 4.48 mmol, internal standard) and catalyst (5 mg 0.819 mol% relative to epoxide) was stirred at room temperature in a 10 mL round-bottomed flask equipped with CO_2 balloon (1 bar pure CO_2 or 15% CO_2 mixed with 85%N_2). After reaction, the catalyst was separated and the resulting solution was further diluted with ethyl acetate. The reactants conversions (using internal standard method) and products yields (measured by standard products samples) were determined by a gas chromatography (Agilent 7890B) equipped with a flame ionization detector and a capillary column (HP-5, 30 m × 0.25 mm × 0.25 μm). The typical conditions were as follows: injection temperature at 220 °C; detection temperature at 240 °C, column temperature at 60 °C for 2 min in the beginning, a ramp of 10 °C min^{-1} to 220 °C and holding at 220 °C for 5 min.

For recycling tests, the reaction was carried out with propylene oxide (40 mmol), tetrabutylammonium bromide (TBAB) (300 mg, 2.34 mol% relative to epoxide), *n*-dodecane (8 mL, internal standard) and catalyst (40 mg, 0.819 mol% relative to epoxide). After reaction, the catalyst was separated by filtration, washed with EtOAc and CH_2Cl_2

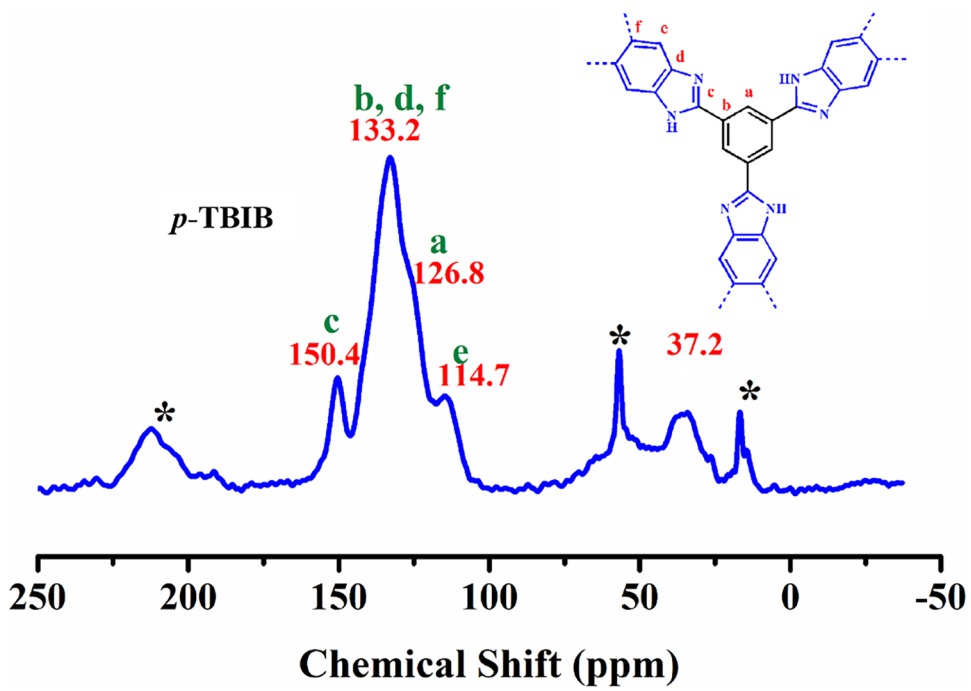

Fig. 1. ^{13}C CP/MAS NMR spectra of *p*-TBIB Asterisk (*) denotes spinning side band (spinning speed = 7.5 kHz)

for three times, respectively and dried d at 80 °C overnight under vacuum. Then, the catalyst was used for the next run with addition of fresh TBAB and propylene oxide.

3 Results and discussion

Firstly, we synthesized 1,3,5-tris(*1H*-benzo[d]imidazol-2-yl) benzene monomer by condensation of trimesoic acid and o-phenylenediamine (Scheme S1). The monomer was confirmed by ^{1}H-NMR (Fig. S1), ^{13}CNMR (Fig. S2) and high resolution mass spectrometry (Fig. S3), the characterization results are agreement with those of reported in literature [37]. Then, 1,3,5-tris(*1H*-benzo[d]imidazol-2-yl)benzene was dissolved in anhydrous dichloromethane and polymerized by a facile Friedel–Crafts alkylation using anhydrous $AlCl_3$ as catalyst. As the procedure shown in Scheme 1, the 1,3,5-tris(*1H*-benzo[d]imidazol-2-yl)benzene molecules can be easily bending to polymeric spheres (*p*-TBIB) under the polymerization process.

We subsequently performed the ^{1}H–^{13}C cross-polarization magic-angle spinning (CP-MAS) ^{13}C NMR spectra to study the structure features at the molecular level (Fig. 1). The peak at ca.150.4 ppm (c) in *p*-TBIB, correspond to NC(Ph)N in benzimidazole units. The existence of aromatic carbons can be confirmed by the peaks at ca.114.7 (e), 126.8

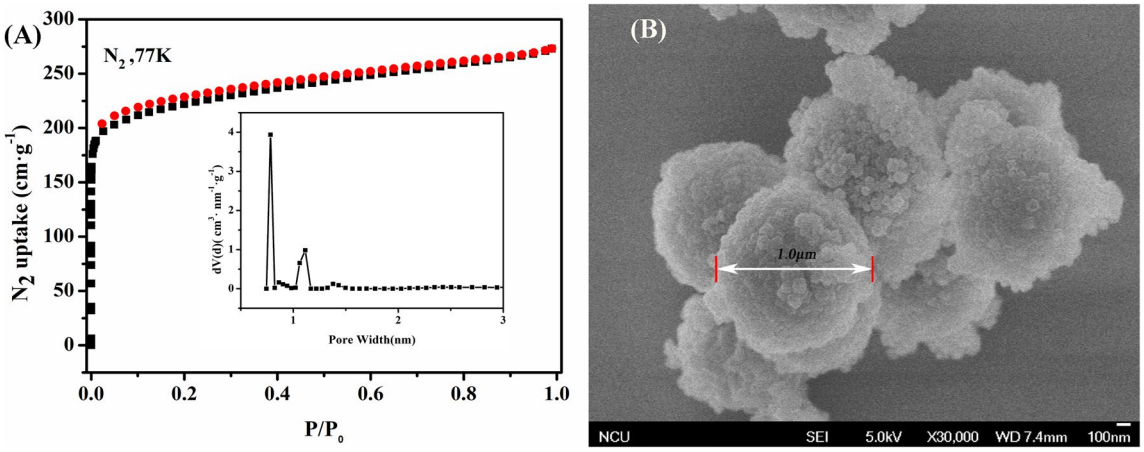

Fig. 2 **a** N_2 adsorption–desorption isotherms with pore size distributions and **b** SEM image of *p*-TBIB

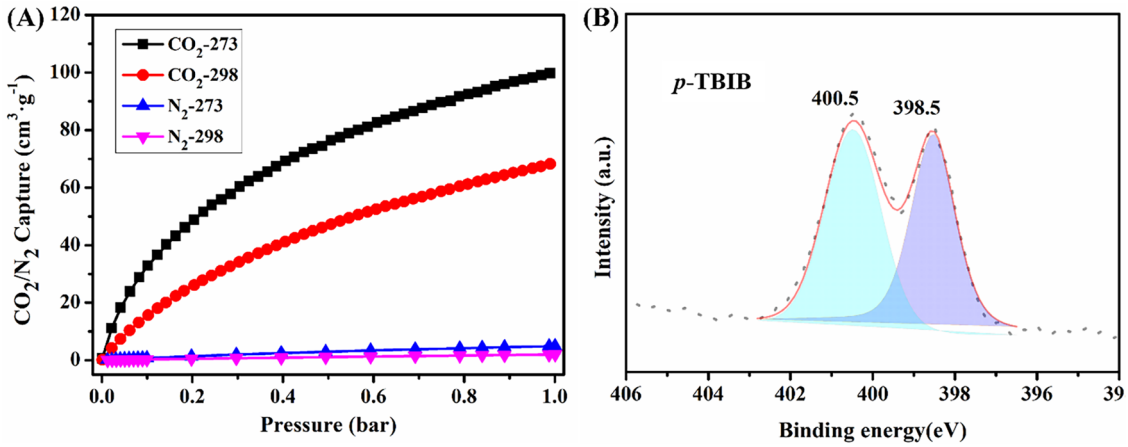

Fig. 3 **a** CO_2/N_2 uptake isotherms of *p*-TBIB at both 273 K and 298 K, up to 1 bar; **b** N 1*s* XPS spectra of *p*-TBIB

(a) and 133.2 ppm (b, d and f) [38]. More importantly, the chemical shift at ca.37.2 ppm is assigned to the methylene carbon [38]. demonstrating the monomer linked like the drawing structure in Fig. 1 and Scheme 1. The existence of free N–H bond can be further evidenced by FT-IR spectra (Fig. S4) at 3415 cm^{-1} both in TBIB monomer and *p*-TBIB [38].

To deeper understand the physical structure of synthesized *p*-TBIB, N_2 adsorption–desorption, powder X-ray diffraction (PXRD) and Scan electron microscopy (SEM) were measured. N_2 adsorption–desorption isotherm of *p*-TBIB (Fig. 2a) was firstly recorded at − 77 K to assess its porous nature. The *p*-TBIB shows typical type-I isotherm with high N_2 uptake at low relative pressure and high abundance of micropores calculated by the nonlocal density functional theory (NLDFT) (< 2 nm). The *p*-TBIB exhibits a high Brunauer–Emmett–Teller (BET) surface area of 840 $m^2\ g^{-1}$ and total pore volume and 1.20 $cm^3\ g^{-1}$ (Table S1), respectively. *p*-TBIB was obtained as an amorphous powder, evidenced by both PXRD pattern (Fig. S5). But the morphology of *p*-TBIB displayed in SEM image (Fig. 2b) is spherical shape with the size estimated to be ca. 1.0 µm. This microporous and spherical polymer usually shows a high gas capture and structural stability due to its high microporosity and optimal shape of nature selection, which further proved by the results of CO_2 uptake and TG curves and solvent dissolving experiment, respectively.

The material (*p*-TBIB) is capable of adsorbing a significant amount of CO_2 molecules under the ambient condition. The CO_2 adsorption isotherms were carefully measured up to 1 bar. As shown in Fig. 3a, the polymer shows uptake capacities as high as 100.8 and 62.7 $cm^3\ g^{-1}$ at 273 and 298 K, respectively. Selectivity is another important parameter for separation applications. In this regard, we further measured N_2 adsorption at 273 K (298 K) to examine the separation ability of *p*-TBIB (Fig. 3a). Only 4.95 (2.0) $cm^3\ g^{-1}$ of N_2 could be adsorbed. The CO_2/N_2 selectivity was then calculated to be as high as 37 (46) at 273 K (298 K) and 1 bar from the ratio of the initial slopes (Table S1 and Fig. S6), comparable with that of benzimidazole-linked polymers BILP-X (1–7) (31–71 at 298 K) [38] and many

Table 1 The cycloaddition of CO_2 with propylene oxide catalyzed by various catalysts at ambient conditions

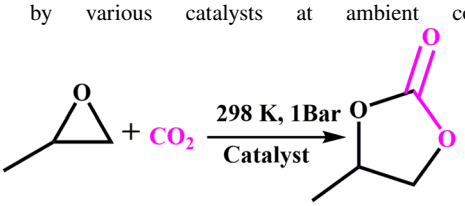

Catalyst	Cocat	Conv. (%)	Selec. (%)	TON[a]	Ref
–	–	0	–	–	This work
–	TBAB	39	> 99	–	This work
PTBP	–	0	–	–	This work
PTBP	TBAB	38	> 99	–	This work
TBIB	–	52	97	215.5	This work
TBIB	TBAB	96	98	181.8	This work
p-TBIB	–	45	> 99	110.0	This work
p-TBIB	TBAB	97	> 99	237.0	This work
Co/POP-TPP	TBAB	95.6	99	433.5	[17]
Co(III)@cage	TBAB	58	> 99	175.7	[18]
Hf-NU-1000 (Cr)	H_4TBAP_y	100	> 99	25	[19]
FJI-H7(Cu)	TBAB	66.5	99	332.5	[20]
MMPF-9(Cu)	TBAB	87.4	99	699.2	[21]
MMCF-2(Cu)	TBAB	95.4	99	756	[22]
Co-CMP	TBAB	81.5	99	167	[23]

Reaction conditions: propylene oxide and CO_2 (1 bar) at 298 K for 24 h

[a]TON = molar of product/molar of catalyst

Table 2 The cycloaddition of CO_2 with various epoxides over the *p*-TBIB catalyst

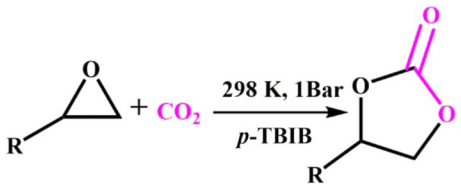

Entry	epoxide	product	Conv. (%)	Select. (%)	Yield (%)	TON
1		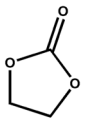	95 (24 h)	> 99	95	232.2
2	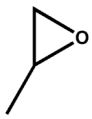	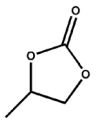	97 (24 h)	> 99	97	237.0
3	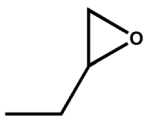	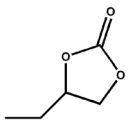	93 (24 h)	> 99	93	227.2
4	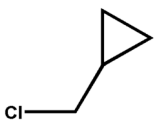	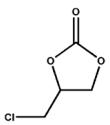	89 (24 h)	> 99	89	217.4
5	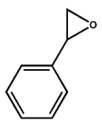	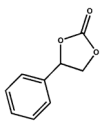	81 (96 h)	> 99	81	197.8
6	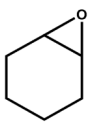	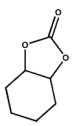	73 (96 h)	> 99	73	178.4
7	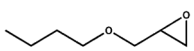	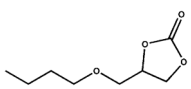	66 (96 h)	> 99	66	161.2

Reaction conditions: epoxide (5 mmol), *p*-TBIB catalyst (5 mg, 0.410 mol%), TBAB (37.6 mg, 2.34 mol%), at 298 K and 1 bar CO_2

other porous organic polymers-based adsorbents [39–41]. We reasoned that high abundance of N-doped sites within the polymeric backbone could play a crucial role in achieving this high selective CO_2 adsorption performance. As a result, we carried out the X-ray photoelectron spectroscopy (XPS) in an effort to gain a better understanding of these CO_2-philic sites (Fig. 3b). To our delight, a high N doping of 14.49 at.% (Table S1) on the surface of the framework was measured, where pyridinic (398.5 eV, 49.7%) and pyrrolic nitrogen (400.5 eV, 50.3%) were the two different nitrogen species [42]. Accordingly, they may serve as binding sites for CO_2 uptake through an electrostatic interaction, and thus highly selective separation performance. The isosteric heats of adsorption (Q_{st}) on *p*-TBIB was also calculated by fitting the CO_2 adsorption isotherms obtained at 273 and 298 K and by applying a variant of the Clausius–Claperyron equation (Fig. S7). At low adsorption values, the polymer exhibits a high adsorption heat of ca. 27 kJ mol^{-1}, which could be attributed to the existence of rich micropores and N-doped CO_2-philic sites [42].

The enrichment of the CO_2 (62.7 cm^3 g^{-1} at 298 K and 1 bar) and N-doped CO_2-philic sites in the nanopores is expected to be beneficial for the promotion of the CO_2 conversion. The cycloaddition of pure CO_2 (1 bar) with propylene oxide (PO) at room temperature (298 K) was selected as a model to start our exploratory experiments. As shown in Table 1. Obviously, no reaction occurred in the absence of any catalyst or with the no imidazole polyemer (1,3,5-triphenylbenzene-linked polymer, PTPB) [43]. Compare to PTPB, the *p*-TBIB displayed a higher propylene oxide

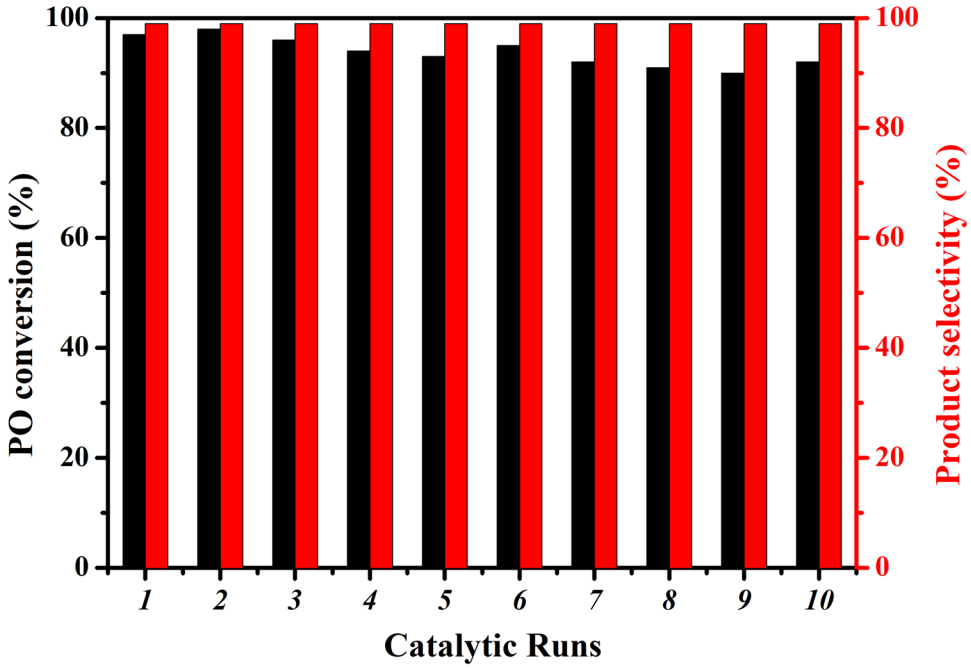

Fig. 4 The reusablity of *p*-TBIB in the cycloaddition of CO_2 with propylene oxide (PO)

conversion (45%, TON: 110.0) and cycloaddition product selectivity (99%). Besides, after the cocatalyst TBAB addition, the conversion increased from 45 to 97% (TON: 237.0), while the conversion of only using the cocatalyst TBAB was 39%. These results indicated that amino-containing electrophiles could interact with the epoxide via hydrogen bonding interaction, thus facilitating the ring opening of propylene oxide. Moreover, the catalytic performance of *p*-TBIB is completely comparable with that of the homogeneous TBIB catalyst and near that of the most active metalated heterogeneous catalysts (Co/POP-TPP [17], Co(III)@cage [18], Hf-NU-1000 [19], Cu-MOF [20–22] and Co-CMP [23]) with the assistant of cocatalyst at ambient conditions. According to the achieved results, a reaction mechanism (Scheme S2) is proposed, the *p*-TBIB first react with PO via hydrogen bonding interaction and then with the assistant of cocatalyst to open the ring. Meanwhile, CO_2 are absorbed and activated on *p*-TBIB. Finally, the product is formed, the catalyst returns to the original state.

Motivated by these promising catalytic results under ambient conditions, the catalyst *p*-TBIB was extended to a scope of epoxides substrates (Table 2). This catalyst is still active for the conversion of these epoxides (conversions: 66–97%, TON numbers: 161.2–237.0), but the activities are strongly dependent on their structures. Clearly, size-dependent catalysis is observed when using the substrates with larger dimensions (Table 2, entries 5–7) which give rise to lower activities.

Due to the emission of CO_2 in industrial processes normally below 15% [26], the cycloaddition was carried out under relatively low CO_2 concentration (15%vol. CO_2 + 85% vol. N_2) should be more significant than that under pure CO_2. Unexpectedly, *p*-TBIB exhibited a higher catalytic performance than that of homogeneous TBIB with or without cocatalyst (Table S2), which was benefit from the high CO_2 capacity and selectivity of *p*-TBIB.

The reusability and stability were the most important performance for an ideal heterogeneous catalyst. The catalyst *p*-TBIB can be reused at least ten times without any significant catalytic activity (over 90%) decrease. (Fig. 4) And the structure was stable under nitrogen atmosphere up to 400 ℃ (Fig. S8) and in many solvents such as ethanol, acetone, DMSO and propylene oxide (Fig. S9).

4 Conclusions

In summary, a metal-free microporous polymeric spheres catalyst was developed by a simple Friedel–Crafts alkylation. The experimental results demonstrated that the high CO_2 uptake (62.7 $cm^3\ g^{-1}$, at 298 K and 1 bar), selectivity over N_2 (46 at 298 K) and the hydrogen bonding interaction with the epoxides of the catalyst can boost the cycloaddition performance under ambient conditions even at ambient conditions. More importantly, the high stable and reusability of the catalyst are benefit from the spherical structure of *p*-TBIB. Besides, the size-dependent catalysis also affects the catalytic performance. According to the achieved results, they might offer the opportunity to design more efficient heterogeneous catalysts under ambient conditions for chemical fixation of CO_2 in the future.

Acknowledgements This work supported by the National Natural Science Foundation of China (No. 21663016), the Key Laboratory of Jiangxi Province For Environment and Energy Catalysis (No. 20181BCD40004), the research project on teaching reform of degree and graduate education of Jiangxi Province (No. JXYJG-2018-007), the project of East China University of Technology of experimental technology research and development (No. DHSYKF-2019-024) and the Opening Project of Jiangxi Province Key Laboratory of Polymer Micro/Nano Manufacturing and Devices (No. PMND201906).

References

1. Zhang L, Zhao Z, Gong J (2017) Angew Chem Int Ed 56:11326
2. Eveloy V (2019) Renew Sust Energ Rev 108:550
3. Yang ZZ, He LN, Gao J, Liu AH, Yu B (2012) Energy Environ Sci 5:6602
4. Omae I (2012) Coord Chem Rev 256:1384
5. Munirah MZ, Abdul RM (2018) Renew Sust Energ Rev 98:56
6. Lu X, Darensbourg DJ (2012) Chem Soc Rev 41:1462
7. Li Y, Cui D, Zhu J, Huang P, Tian Z, Jia Y, Wang P (2019) Green Chem 21:5231
8. Zhang S, Sun J, Zhang X, Xin J, Miao Q, Wang J (2014) Chem Soc Rev 43:7838
9. Paddock RL, Nguyen ST (2001) J Am Chem Soc 123:11498
10. Lu X, Zhang Y, Jin K, Luo L, Wang H (2004) J Catal 227:537
11. Wu X, North M (2017) Chemsuschem 10:74
12. Ema T, Miyazaki Y, Koyama S, Yano Y, Sakai T (2012) Chem Commun 48:4489
13. Ema T, Miyazaki Y, Shimonishi J, Maeda C, Hasegawa J (2014) J Am Chem Soc 136:15270
14. Qin Y, Guo H, Sheng X, Wang X, Wang F (2015) Green Chem 17:2853
15. Maeda C, Taniguchi T, Ogawa K, Ema T (2015) Angew Chem Int Ed 54:134
16. Liang J, Huang Y, Cao R (2019) Coord Chem Rev 378:32
17. Dai Z, Sun Q, Liu X, Bian C, Wu Q, Pan S, Wang L, Meng X, Deng F, Xiao FS (2016) J Catal 338:202
18. Ng CK, Toh RW, Lin TT, Luo H, Hor TA, Wu J (2019) Chem Sci 10:1549
19. Beyzavi MH, Klet RC, Tussupbayev S, Borycz J, Vermeulen NA, Cramer CJ, Stoddart J, Hupp JT, Farha OK (2014) J Am Chem Soc 136:15861
20. Zheng J, Wu M, Jiang F, Su W, Hong M (2015) Chem Sci 6:3466
21. Gao W, Wojtas L, Ma S (2014) Chem Commun 50:5316
22. Gao W, Chen Y, Niu Y, Williams K, Cash L, Perez PJ, Wojtas L, Cai J, Chen Y, Ma S (2014) Angew Chem Int Ed 53:2615
23. Xie Y, Wang T, Liu X, Zou K, Deng W (2013) Nat Commun 4:1
24. Bondarenko GN, Dvurechenskaya EG, Ganina OG, Alonso F, Beletskaya IP (2019) Appl Catal B 254:380
25. Yu S, Liu X, Ma J, Niu Z, Cheng P (2016) J CO2 Util 14:122
26. Bae YS, Snurr RQ (2011) Angew Chem Int Ed 50:11586
27. Ding S, Wang W (2013) Chem Soc Rev 42:548
28. Feng X, Ding X, Jiang D (2012) Chem Soc Rev 41:6010
29. Dawson R, Adams DJ, Cooper AI (2011) Chem Sci 2:1173
30. Tan L, Tan B (2017) Chem Soc Rev 46:3322
31. Qiu P, Ma B, Hung C, Li W, Zhao D (2019) Acc Chem Res 52:2928
32. Zhang W, Mei Y, Wu P, Wu H, He M (2019) Catal Sci Technol 9:1030
33. Steinbauer J, Werner T (2017) Chemsuschem 10:3025
34. Wang T, Song X, Luo Q, Yang X, Chong S, Zhang J, Ji M (2018) Microporous Mesoporous Mater 267:84
35. Sun J, Wang J, Cheng W, Zhang J, Li X, Zhang S, She Y (2012) Green Chem 14:654
36. Zhang W, Wang Q, Wu H, Wu P, He M (2014) Green Chem 16:4767
37. Xiong J, Li J, Mo G, Huo J, Liu J, Chen X, Wang Z (2014) J Org Chem 79:11619
38. Rabbani MG, El-Kaderi HM (2012) Chem Mater 24:1511
39. Zhu X, Ding S, Abney CW, Browning KL, Sacci RL, Veith GM, Tian C, Dai S (2017) Chem Commun 53:7645
40. Zhu X, Tian C, Jin T, Browning KL, Sacci RL, Veith GM, Dai S (2017) ACS Macro Lett 6:1056
41. Zhu X, Tian C, Jin T, Wang J, Mahurin SM, Mei W, Xiong Y, Hu J, Feng X, Liu H (2014) Chem Commun 50:15055
42. Zhu X, Tian C, Veith GM, Abney CW, Dehaudt J, Dai S (2016) J Am Chem Soc 138:11497
43. Xu S, Luo Y, Tan B (2013) Macromol Rapid Commun 34:471

Affiliations

Shunmin Ding[1] · Ling Sun[1] · Xiaohua Ma[1] · Dan Cheng[1] · Shaohua Wu[1] · Rong Zeng[2] · Shengjun Deng[1] · Chao Chen[1] · Ning Zhang[1]

[1] Key Laboratory of Jiangxi Province for Environment and Energy Catalysis, College of Chemistry, Nanchang University, Nanchang 330031, Jiangxi, People's Republic of China

[2] Jiangxi Province Key Laboratory of Polymer Micro/Nano Manufacturing and Devices, School of Chemistry, Biology and Materials Science, East China University of Technology, Nanchang 330013, People's Republic of China